

# NJC

Accepted Manuscript



This is an *Accepted Manuscript*, which has been through the Royal Society of Chemistry peer review process and has been accepted for publication.

*Accepted Manuscripts* are published online shortly after acceptance, before technical editing, formatting and proof reading. Using this free service, authors can make their results available to the community, in citable form, before we publish the edited article. We will replace this *Accepted Manuscript* with the edited and formatted *Advance Article* as soon as it is available.

You can find more information about *Accepted Manuscripts* in the [Information for Authors](#).

Please note that technical editing may introduce minor changes to the text and/or graphics, which may alter content. The journal's standard [Terms & Conditions](#) and the [Ethical guidelines](#) still apply. In no event shall the Royal Society of Chemistry be held responsible for any errors or omissions in this *Accepted Manuscript* or any consequences arising from the use of any information it contains.



[www.rsc.org/njc](http://www.rsc.org/njc)

## ARTICLE

# Enhancing the electronic properties and quantum efficiency of sulfonyl/phosphoryl-substituted blue iridium complexes via different ancillary ligands

Cite this: DOI: 10.1039/x0xx00000x

Yanling Si<sup>a</sup>, Shuai Zhang<sup>a</sup>, Nan Qu<sup>a</sup>, Guoyou Luan<sup>\*a</sup> and Zhijian Wu<sup>\*b</sup>

Received 00th January 2012,

Accepted 00th January 2012

DOI: 10.1039/x0xx00000x

www.rsc.org/

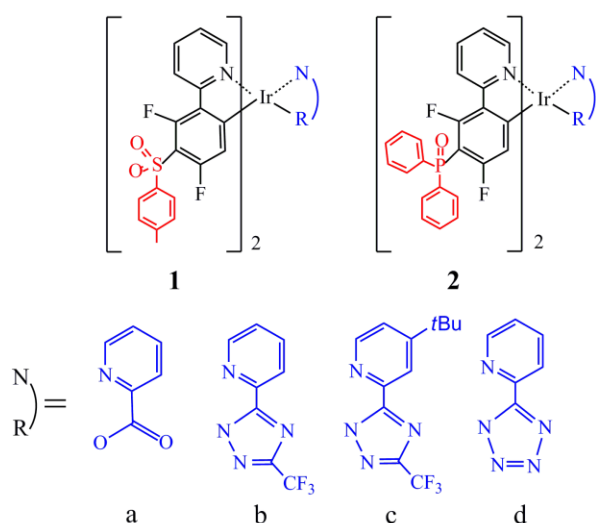
DFT/TDDFT investigation was performed on the electronic structures, absorption and emission properties, as well as the phosphorescence efficiency of recent synthesized Ir(III) complexes SOFIrpic (**1a**) and POFIrpic (**2a**) with sulfonyl/phosphoryl substituted 2-(2,4-difluorophenyl)pyridine(dfppy) as the cyclometalated ligands. The calculated absorption and emission wavelengths are in agreement with experimental data. Compared with **2a**, the higher quantum yield of experimental observation for **1a** was explained by its smaller energy separation between the singlet S<sub>1</sub> and the triplet T<sub>3</sub> states. Based on these experimental structures, a series of cyclometalated Ir(III) complexes (**1b**, **1c**, **1d** and **2b**, **2c**, **2d**) have been designed by introducing different ancillary ligands. The calculated results reveal that the different ancillary ligands not only tune the energy gap but also enhance the photoluminescence quantum efficiency. It is expected that the designed **1b**, **2b** and **2c** could be potential candidates as blue-emitting materials with high quantum efficiency.

## 1. Introduction

Organometallic iridium(III) complexes have been widely studied in recent years for their potential applications in organic light emitting diodes (OLEDs), luminescent biological-labeling reagents, molecular sensor for hypoxia detection and light emitting electrochemical cells (LECs).<sup>1-8</sup> One unique feature of the iridium (III) complexes that contributes to these applications is the strong spin-orbit coupling caused by heavy metal ions, which results in efficient intersystem crossing from the singlet to the triplet excited state. Mixing of the singlet and triplet excited states not only removes the spin-forbidden nature of the radiative relaxation of the triplet state, but also significantly shortens the triplet state lifetime. Thus, higher phosphorescent efficiencies can be achieved.<sup>9-13</sup> Another reason for the growing attention on iridium (III) complexes is that the emission can be tuned to cover the range of colors from red and green to blue. Of these three colors of emitters, phosphorescent

red and green emitters are widely available on the market. However, there is still a lack of stable and efficient blue-emitting OLEDs, which are essential for the commercial launch of devices for lighting. Lots of efforts have been done to shift the emission wavelength of organometallic complexes to the blue spectral region, while maintaining high photoluminescence quantum efficiency ( $\Phi_{PL}$ ).<sup>14-20</sup> This is a challenging task because blue-emitting materials with high efficiency and good stability require the wide energy gap between the excited triplet state and the ground state.

Recently, Yang et al.<sup>21</sup> reported two iridium complexes, SOFIrpic (**1a**) and POFIrpic (**2a**) with sulfonyl/phosphoryl substituted 2-(2,4-difluorophenyl)pyridine(dfppy) as the cyclometalated ligands (Scheme 1). The sulfonyl (S=O) and phosphoryl (P=O) moieties are strong electron-withdrawing groups and tune the emission of iridium complex to the blue region with quantum yields of 55% and 49%, respectively.



**Scheme 1** Chemical structures of the investigated complexes (**a**: picolinate (pic); **b**: 3-(trifluoromethyl)-5-(pyridine-2-yl)-1,2,4-triazolate (taz); **c**: 4-tert-butyl-2-(5-(trifluoromethyl)-2H-1,2,4-triazol-3-yl)pyridine (bptz); **d**: 5-(pyridine-2-yl)-1H-tetrazolate(pyN4)).

In this work, based on the synthesized complexes **1a** and **2a**, the complexes **1b**, **1c**, **1d** and **2b**, **2c**, **2d** with sulfonyl/phosphoryl substituted 2-(2,4-difluorophenyl)pyridine(dfppy) as the cyclometalated ligands (Scheme 1) were designed to understand the structure-property relationship of the iridium complexes, which is important in the development of novel OLED devices. We present density functional theory (DFT) calculations on the ground and excited state geometries, the frontier molecular orbitals (FMOs), and the electronic absorptions and emission spectra. Furthermore, we also investigated the influence of the different ligands on the photoluminescence quantum efficiency of these Ir (III) complexes, which will be of great benefit for designing highly efficient blue-emitting Ir (III) complexes.

## 2. Computational method

The ground state and the lowest-lying triplet excited state geometries for each complex were optimized by using the density functional theory (DFT)<sup>22</sup> with the hybrid-type Perdew-Burke-Ernzerhof exchange correlation functional (PBE0) and the unrestricted PBE0 (UPBE0),<sup>23</sup> respectively, which have been proved to be efficient and accurate for the calculation of transition metal complexes.<sup>24-26</sup> To ensure the accuracy of the

calculation method, three methods (PBE0, B3LYP<sup>27</sup> and M062X<sup>28</sup> level) were used to optimize the geometry structural of the complex **1a** (Table S1, Supporting Information). It was found that the PBE0 functional is more precise for the optimization of the studied complex. There were no symmetry constraints on the studied complexes during the geometry optimization. Vibrational frequencies were calculated to confirm that each configuration was a minimum on the potential energy surface. In addition, single-point calculations were performed at the optimized ground state geometries of these complexes for the molecule orbital population.

The absorption and emission properties in CH<sub>2</sub>Cl<sub>2</sub> media were calculated by time-dependent density functional theory (TDDFT)<sup>29</sup> associated with the polarized continuum model (PCM).<sup>30</sup> Due to the problem of TDDFT in calculating the charge transfer excited states, three different functionals (PBE0, B3LYP, and M062X) were performed to study the emission spectra of **1a** and **2a**. Our results indicated that for the studied complexes, M062X is more accurate in reproducing the experimental data (Table S2). Therefore, it was selected in the calculation of emission spectra.

The “double- $\xi$ ” quality basis set LANL2DZ<sup>31</sup> associated with the pseudopotential was employed on atom Ir. The 6-31G(d)<sup>32</sup> basis set was used for non-metal atoms in the gradient optimizations. All calculations were performed with the Gaussian 09 software package.<sup>33</sup> GaussSum 2.5<sup>34</sup> was used for orbital and UV/Vis spectra analysis and Molekel 4.3.2 user interface<sup>35</sup> was used to manipulate the structures and orbitals.

## 3. Results and discussion

### 3.1. Geometries in the ground and the lowest-lying triplet excited state

The schematic structures of the investigated complexes are presented in Scheme 1 and the optimized ground state structures of **1a** and **2a** are shown in Fig. 1, along with the numbering of some key atoms.

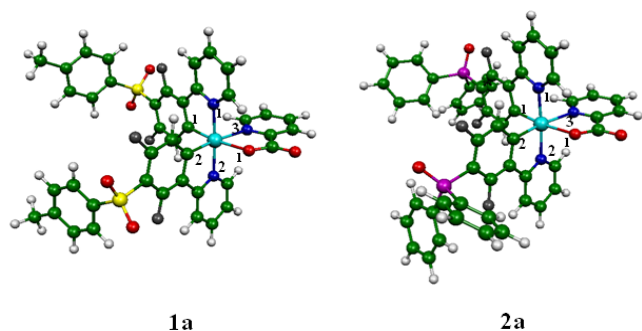


**Fig. 1** Optimized structures for **1a** and **2a** in the  $S_0$  state: the Ir, S, P, N, O, C, F and H atoms are displayed in blue-sky, yellow, purple, blue, red, green, gray and white colors, respectively.

The bond distances between Ir metal and coordinating atoms of the studied complexes in ground state ( $S_0$ ) and lowest triplet excited state ( $T_1$ ) are summarized in Table 1, together with the X-ray crystal structure data of **1a**. Generally speaking, the calculated bond lengths of **1a** are in good agreement with the corresponding experimental values, with the largest discrepancy of 0.023 Å found in Ir-N2 bond length.

As the ligands in the studied complexes change, a clear influence is found in the bond lengths in the ground state. For **1a-1d** (**1a-1d** indicates the complexes **1a**, **1b**, **1c** and **1d**, the same hereafter), the Ir-N1, Ir-C1 and Ir-N3 bond lengths of the **1b-1d** are elongated by 0.01-0.04 Å compared with **1a**. On the other hand, the Ir-N2 and Ir-C2 bond lengths remain practically unchanged. It is interesting to note that Ir-N4 bond lengths of **1b**, **1c** and **1d**, specifically for **1b**, are significantly shortened compared with the Ir-O1 bond length on the picolinate ligand in the complex **1a**. The shortened Ir-N4 bond lengths are expected to enhance the coordination interaction between the Ir(III) center and ancillary ligands, which may also increase the probability of charge transfer from metal to ancillary ligands. The same observation can be made when comparing **2b-2d** to **2a**.

For the lowest excited state, the Ir-N1, Ir-C1 and Ir-C2 bond lengths of **1a-1c** and **2a** as well as **2b** are greatly contracted compared with those in the  $S_0$  state, while the Ir-N1 bond lengths of **1d**, **2c** and **2d** are elongated. Meanwhile, the Ir-N2 bond length of **1a-1c**, **2a** and **2b** are found to be slightly

Table 1 Main optimized bond lengths of the studied complexes in the ground and the lowest lying triplet states at PBE0/LANL2DZ level

	<b>1a</b>		<b>1b</b>		<b>1c</b>		<b>1d</b>	
	$S_0$	$T_1$	$S_0$	$T_1$	$S_0$	$T_1$	$S_0$	$T_1$
Ir-N1	2.037	2.015	2.046	2.019	2.046	2.018	2.047	2.056
Ir-C1	1.986	1.969	2.003	1.987	2.002	1.986	2.000	2.000
Ir-C2	1.992	1.988	1.991	1.988	1.991	1.989	1.991	1.979
Ir-N2	2.048	2.059	2.050	2.060	2.049	2.060	2.049	2.023
Ir-N3	2.163	2.184	2.206	2.223	2.202	2.217	2.211	2.213
Ir-O1 (N4)	2.149	2.143	2.116	2.122	2.117	2.123	2.120	2.126
	<b>2a</b>		<b>2b</b>		<b>2c</b>		<b>2d</b>	
	$S_0$	$T_1$	$S_0$	$T_1$	$S_0$	$T_1$	$S_0$	$T_1$
Ir-N1	2.037	2.016	2.046	2.019	2.046	2.057	2.047	2.057
Ir-C1	1.986	1.968	2.002	1.987	2.002	2.001	2.000	2.000
Ir-C2	1.992	1.987	1.991	1.988	1.991	1.979	1.990	1.978
Ir-N2	2.048	2.059	2.049	2.059	2.049	2.020	2.050	2.024
Ir-N3	2.165	2.187	2.207	2.223	2.201	2.204	2.211	2.214
Ir-O1 (N4)	2.153	2.146	2.120	2.124	2.121	2.125	2.123	2.129

elongated by  $\sim 0.01$  Å upon excitation. For **1d**, **2c** and **2d**, significantly shortening is observed for Ir-C2 and Ir-N2 in the  $T_1$  state compared to the  $S_0$  state, see Table 1. The subtle difference in bond lengths can be ascribed to the different structures between the singlet ground state and the triplet excited state.

### 3.2 Frontier molecular orbital Properties

Herein, we will discuss the frontier molecular orbitals (FMOs) with a special emphasis on the HOMO (highest occupied molecular orbital) and LUMO (lowest unoccupied molecular orbital) distribution and energy gaps, since the TDDFT calculations reveal that the first triplet ( $S_0 \rightarrow T_1$ ) excited states primarily involve the electronic transition between these two orbitals. The contour plots of HOMO and LUMO and energy gaps are displayed in Fig. 2. The detailed information of molecular orbital, including compositions, energies of metal and ligand orbitals are listed in Tables S3–S10, respectively.

For **1a**, the LUMO is primarily composed of one SOF ligand ( $\sim 85\%$ ) with small contribution from picolinate ligand ( $\sim 11\%$ ). For **1b-1d**, the LUMOs are also mainly localized on the SOF ligand ( $>89\%$ ), indicating that the LUMO distribution are hardly influenced by the variation of ancillary ligands. It is clear that the HOMOs of **1a-1d** are predominantly contributed by the Ir (III) center and the phenyl parts of the SOF ligands.

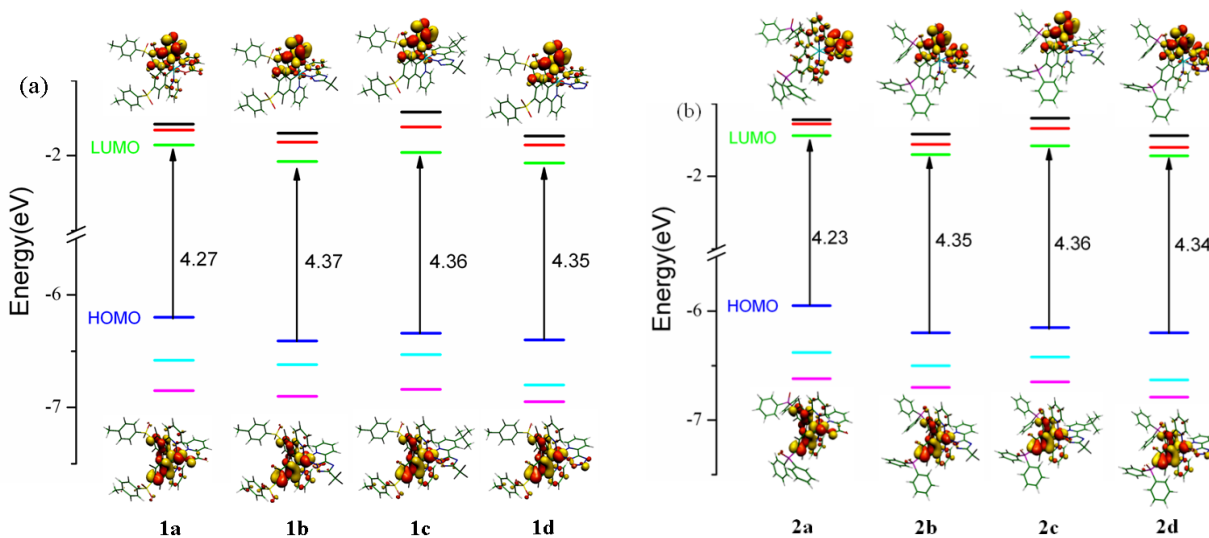


**Fig. 2** Energy levels, energy gaps (in eV), and HOMO and LUMO surfaces for the studied complexes.

However, it is interesting to note that changing the ancillary ligands makes the composition of LUMOs of **2a-2d** varied greatly. From Fig. 2, we can see that the LUMO of **2a** is mainly composed of the pic ancillary ligand, whereas only 28% of the taz ancillary ligand and 31% of the pyN4 ancillary ligand have contributions to the LUMOs of **2b** and **2d**. Moreover, the LUMO of **2c** have even much smaller amount of electron density on the bptz ancillary ligand (~ 4%).

The different ancillary ligands in these complexes have a significant effect on the energy levels as shown in Fig. 2. Compared with complex **1a**, the energy level of HOMO of **1b-1d** are lowered more than that of LUMO, leading to the energy gap of HOMO–LUMO is increased by 0.10 eV, 0.09 eV and 0.08 eV compared with that of **1a**. For complexes **2b-2d**, the stabilization of HOMO are relatively larger than that of LUMO, so the HOMO–LUMO energy gap of **2b-2d** is also increases compared with that of **2a** ( by 0.12 eV, 0.13 eV and 0.11 eV, respectively).

### 3.3 Absorption spectra

TDDFT method is widely used to calculate the absorption properties of Ir(III) complexes on the basis of the optimized geometries.<sup>36</sup> Here, the TDDFT/B3LYP method with PCM in

CH<sub>2</sub>Cl<sub>2</sub> was used to calculate the absorption properties of the studied complexes. The absorption energies, dominant configurations, and transition nature of the selected excited states with large oscillator strengths (*f*) for **1a-1d** are listed in Table 2 (for **2a-2d** see Table S3), along with the experimental data for **1a** and **2a**. The lowest singlet absorptions at 374 and 379 nm are in good agreement with the experimental values at 372 and 374 nm for **1a** and **2a**, respectively, which means that our calculated absorption data can well reproduce the experimental ones.

The results in Table 2 show that the lowest singlet transition of complex **1a** is contributed mainly by HOMO → LUMO transition. According to our calculation, the transition character of **1a** can be assigned as metal to ligand charge transfer (MLCT)/ intraligand charge transfer (ILCT)/ligand to ligand charge transfer (LLCT). For **1b**, **1c** and **1d**, although the lowest singlet transitions are similar to complex **1a**, the transition characters are different, which are assigned as MLCT/ILCT, due to the different ancillary ligands. Moreover, the lowest singlet absorptions of **1a**, **1b**, **1c** and **1d** are at 374, 361, 362 and 360 nm, respectively. This indicates that the taz, bptz and pyN4 ligands induce blue shift of the absorption bands of **1b**, **1c** and **1d** relative to **1a**. The same observation can be made

Table 2 Calculated wavelength (nm), oscillator strength (*f*) and dominant orbital excitations of the lowest singlet and triplet absorptions for **1a-1d**

	state	$\lambda_{\text{cal}}$	<i>f</i>	Configuration	Character	Exp. <sup>21</sup>
<b>1a</b>	S <sub>1</sub>	374	0.0578	HOMO->LUMO (91%)	MLCT/ILCT/LLCT	372
	S <sub>2,1</sub>	282	0.1965	H-4->L+1 (26%),	MLCT/ILCT/LLCT	
				H-3->L+1 (14%),	MLCT/ILCT/LLCT	
				H-3->L+2 (13%),	MLCT/ILCT/LLCT	
			HOMO->L+5 (27%)	MLCT/ILCT/LLCT		
	T <sub>1</sub>	421	0.0000	HOMO->LUMO (44%)	MLCT/ILCT/LLCT	
<b>1b</b>	S <sub>1</sub>	361	0.0393	HOMO->LUMO (92%)	MLCT/ILCT	
	S <sub>1,8</sub>	284	0.1607	H-3->L+2 (21%),	MLCT/ILCT/LLCT	
				H-1->L+3 (30%)	MLCT/ILCT	
	T <sub>1</sub>	417	0.0000	H-3->LUMO (11%),	MLCT/ILCT	
H-2->LUMO (12%),				ILCT		
H-2->L+1 (12%),				ILCT/LLCT		
			HOMO->LUMO (36%)	MLCT/ILCT		
<b>1c</b>	S <sub>1</sub>	362	0.0393	HOMO->LUMO (94%)	MLCT/ILCT	
	S <sub>2,4</sub>	275	0.2193	H-1->L+4 (26%),	MLCT/ILCT/LLCT	
				H-1->L+6. (16%)	MLCT/ILCT/LLCT	
	T <sub>1</sub>	417	0.0000	H-2->LUMO (12%),	ILCT/LLCT	
H-2->L+1 (11%),				ILCT/LLCT		
			HOMO->LUMO (38%)	MLCT/ILCT		
<b>1d</b>	S <sub>1</sub>	360	0.0463	HOMO->LUMO (89%)	MLCT/ILCT	
	S <sub>2,2</sub>	274	0.2182	HOMO->L+5 (49%)	MLCT/ILCT/LLCT	
	T <sub>1</sub>	417	0.0000	H-2->LUMO (15%),	MLCT/ILCT/LLCT	
HOMO->LUMO (36%)				MLCT/ILCT		

when comparing **2b**, **2c** and **2d** to **2a**. This is consistent with the trend of the HOMO-LUMO energy gaps. Furthermore, for complexes **2a** and **2d**, the lowest singlet transition comes from HOMO→LUMO and HOMO→LUMO+1 with the absorption band at 379 and 364 nm and the character of MLCT/ILCT/LLCT. The lowest absorption bands of **2b** and **2c** are localized at 365 nm and the excitation of HOMO→LUMO is assigned to the character of MLCT/ILCT/LLCT and MLCT/ILCT, respectively.

The complexes **1a** and **2a** have the weak long wavelength absorptions at 445 nm and 447 nm in experiment, which can be assigned to the MLCT transitions<sup>21</sup>. According to Table 2, the calculated lowest triplet absorption of **1a** is at 421 nm, with the primary transition HOMO→LUMO and the characters is MLCT/ILCT/LLCT. For **2a**, the transition HOMO→LUMO, HOMO-1→LUMO+2 and HOMO→LUMO+1 contribute to

the 427 nm absorption and the character can be described as MLCT/ILCT/LLCT. The calculated lowest triplet absorptions of **1b-1d** are at 417 nm with mixed characters of MLCT/ILCT/LLCT. As for **2b-2d**, the calculated T<sub>1</sub> absorptions are at 420 nm and 419 nm. The transition characters are also MLCT/ILCT/LLCT. This non-negligible MLCT is beneficial for efficient intersystem crossing and thus enhance the quantum efficiency for these Ir(III) complexes.

### 3.4 Phosphorescence spectra

As mentioned in the computational method, the phosphorescence properties of the studied complexes were calculated at M062X functional in CH<sub>2</sub>Cl<sub>2</sub> media, on the basis of the optimized lowest triplet excited-state geometries. The calculated emission wavelength, dominant configurations as well as the transition nature are listed in Table 3. The calculated

Table 3 Calculated phosphorescent emission wavelength (in nm) in CH<sub>2</sub>Cl<sub>2</sub> media with the TDDFT method, along with experimental values

	$\lambda_{cal}$	Configuration	Character	Exp. <sup>21</sup>
<b>1a</b>	460	H-1->LUMO (26%), HOMO->LUMO (63%)	MLCT/ILCT/LLCT MLCT/ILCT/LLCT	459
<b>1b</b>	473	H-1->LUMO (12%), HOMO->LUMO (76%)	MLCT/ILCT/LLCT MLCT/ILCT	
<b>1c</b>	472	H-1->LUMO (11%), HOMO->LUMO (75%)	MLCT/ILCT/LLCT MLCT/ILCT	
<b>1d</b>	471	HOMO->LUMO (82%)	MLCT/ILCT	
<b>2a</b>	461	H-1->LUMO (27%), HOMO->LUMO (63%)	MLCT/ILCT/LLCT MLCT/ILCT/LLCT	460
<b>2b</b>	471	H-1->LUMO (20%), HOMO->LUMO (71%)	MLCT/ILCT/LLCT MLCT/ILCT/LLCT	
<b>2c</b>	469	HOMO->LUMO (81%)	MLCT/ILCT	
<b>2d</b>	469	H-1->LUMO (11%), HOMO->LUMO (82%)	MLCT/ILCT/LLCT MLCT/ILCT/LLCT	

emission wavelengths for **1a** and **2a** at M062X level are localized at 460 and 461 nm, which is close to the experimental values at 459 and 460 nm.<sup>21</sup>

As shown in Table 3, the calculated emission wavelengths of **1b-1d** and **2b-2d** (at ~ 470 nm) red shifted by 10 nm compared to **1a** and **2a**. With regard to **1a**, the emission is contributed by transitions from HOMO→LUMO and HOMO-1→LUMO. According to our calculation, the HOMO is localized on Ir (39%) and SOF ligand (55%), the LUMO is mainly from SOF ligand (85%) and pic (11%), the H-1 is localized on Ir (47%), SOF ligand (23%) and pic (29%). Therefore, this emission can be assigned as MLCT/ILCT/LLCT. Table 3 also shows that the nature of the phosphorescence for **1b** and **1c** as well as **2a**, **2b**, **2d** are similar to that of **1a**, which is from the HOMO→LUMO and HOMO-1→LUMO transition with the mixed characters of MLCT/ILCT/LLCT. As for **1d** and **2c**, the emissions are mainly from the HOMO→LUMO. The HOMOs are from d(Ir)+π(SOF) and d(Ir)+π(POF), while the LUMOs are π\*(SOF) and π\*(POF), respectively. Thus, the emissions can be assigned as MLCT/ILCT.

### 3.5 Quantum efficiency

The emission quantum yield ( $\Phi_{PL}$ ) is linked to the radiative ( $k_r$ ) and nonradiative ( $k_{nr}$ ) rate constants, which can be expressed by the following equation, where  $\tau_{em}$  is the emission decay time:

$$\Phi_{PL} = k_r \tau_{em} = \frac{k_r}{k_r + k_{nr}} \quad (1)$$

Clearly, the larger  $k_r$  and smaller  $k_{nr}$  make the complexes have a higher  $\Phi_{PL}$ . As we can see from Table 4, although the  $k_{nr}$  value of **2a** is slightly smaller than that of **1a**, the  $\Phi_{PL}$  of **2a** is lower than that of **1a**. However, the  $k_r$  value of **1a** is significantly larger than that of **2a**. Thus, the larger  $k_r$  seems to be the critical factor of the higher quantum yield for **1a** compared to **2a**.

According to the Einstein theory of spontaneous emission,  $k_r$  is proportional to  $(E_{T1})^3 |M_{T-S}|^2$ ,<sup>37</sup> where  $E_{T1}$  is the emitting energy and  $M_{T-S}$  is the transition dipole moment from the triplet state. Table 4 shows that the emitting energy of **1a** and **2a** are close to each other while the  $k_r$  values are different, indicating that  $E_{T1}$  is not a determining factor. Thus, the transition dipole moment  $|M_{T-S}|$  seems to play a much more important role in controlling the  $k_r$  of the studied complexes. Since the transition metal center is the key that allows the admixture of emissive singlet states into the lowest triplet states, then giving rise to the phosphorescence of these transition metal complexes, we herein correlate  $k_r$  to the spin-orbit coupling (SOC) effects in the emission process.

The heavy atom participation, such as iridium, is believed to increase SOC effects and intersystem crossing (ISC), provided that its orbitals make a significant contribution in the excited states involved. The SOC effects can be elucidated mainly from two aspects. One is the contribution of MLCT in the  $T_1$  state.<sup>38</sup> An increase of MLCT character could enhance SOC and hence the transition probability which would result in a drastic decrease of the radiative lifetime.<sup>39</sup> A large MLCT contribution is then beneficial to increase the  $k_r$ . In Table 4, we list the MLCT contributions for the studied complexes. It is found that relatively high  $k_r$  value of **1a** ( $2.89 \times 10^5 \text{ s}^{-1}$ ) compared with **2a** ( $2.13 \times 10^5 \text{ s}^{-1}$ ) cannot be rationalized by nearly the same MLCT% of **1a** (38.3%) compared with that of **2a** (38.8%).

Secondly, the SOC effects also can be elucidated by the  $S_1-T_1$  energy gap ( $\Delta E_{S1-T1}$ ).<sup>40,41</sup> The  $S_1-T_1$  intersystem crossing (ISC) rate due to SOC interaction plays an important role in the

Table 4 The metal-based charge transfer character (MLCT)(%), singlet-triplet splitting ( $\Delta E_{S_1-T_1}$  in eV) and the transition dipole moment in  $S_0 \rightarrow S_1$  transition ( $\mu_{S_1}$  in D), along with experimental  $\Phi_{PL}$ ,  $k_r$  and  $k_{nr}$

	<b>1a</b>	<b>1b</b>	<b>1c</b>	<b>1d</b>	<b>2a</b>	<b>2b</b>	<b>2c</b>	<b>2d</b>
MLCT	38.3	31.1	30.9	31.0	38.8	32.1	32.0	31.8
$E_{T_1}$	2.69	2.62	2.62	2.63	2.69	2.63	2.64	2.64
$\Delta E_{S_1-T_1}$	0.865	0.983	0.980	1.023	0.848	0.972	0.9878	1.003
$\Delta E_{S_1-T_2}$	0.154	0.183	0.181	0.239	0.170	0.213	0.2238	0.239
$\Delta E_{S_1-T_3}$	-0.097	-0.015	-0.099	-0.118	-0.103	-0.020	-0.0708	-0.131
$\Delta E_{S_1-T_4}$	-0.421	-0.152	-0.150	-0.164	-0.439	-0.127	-0.1504	-0.149
$\Phi_{PL}(\%)^a$	55				49			
$k_r(s^{-1})^b$	$2.89 \times 10^5$				$2.13 \times 10^5$			
$k_{nr}(s^{-1})^c$	$2.37 \times 10^5$				$2.22 \times 10^5$			

<sup>a</sup> ref. 21; <sup>b</sup> $k_r = \Phi_{PL}/\tau$ ; <sup>c</sup> $k_{nr} = (1 - \Phi_{PL})/\tau$  from ref. 21.

phosphorescent process. Therefore, we focus on the singlet  $\rightarrow$  triplet ISC rate to get further insight into the different  $k_r$  of these complexes. A qualitative description of the ISC rate can be performed as a function of the energy separation between the singlet  $S_1$  and the closest triplet  $T_n$ ,<sup>42,43</sup> since the ISC rate exponentially decreases as the singlet-triplet gap increases.<sup>44</sup> Then a minimal  $\Delta E_{S_1-T_n}$  is favorable for enhancing the ISC rate, leading to an increased  $k_r$ . Table 4 shows a slightly larger  $\Delta E_{S_1-T_1}$  for **1a** (0.865 eV) compared with **2a** (0.848 eV), indicating that the  $\Delta E_{S_1-T_1}$  values cannot elucidate the different  $k_r$ . On the other hand, we also note that the  $T_3$  state is the closest to the  $S_1$  state for all the studied complexes, resulting in the largest contribution from  $S_1-T_3$  to the total ISC rate. The significantly smaller  $\Delta E_{S_1-T_3}$  value of **1a** accounts for the larger  $k_r$  compared with **2a**. Thus,  $\Delta E_{S_1-T_3}$  seems to be an important parameter to explain the higher quantum efficiency of **1a** compared to **2a**. In Table 3, it is also found that the  $\Delta E_{S_1-T_1}$  of **1b**, **2b** and **2c** are relatively smaller than that of **1a** and **2a**, indicating that taz and bptz ligands as ancillary chelate in **1b**, **2b** and **2c** are beneficial to enhance the ISC rate, and thus might increase  $k_r$ . Of course, we should remember that besides the factors discussed above, other factors may also affect  $\Phi_{PL}$  which are not taken into account in our discussion.

#### 4. Conclusions

DFT/TDDFT investigations were carried out on the electronic and photophysical properties of recently synthesized blue-emitting Ir(III) complexes SOFIrpic (**1a**) and POFIrpic (**1b**). By introducing different ancillary ligands, a series of Ir(III) complexes **1b-1d** and **2b-2d** based on the experimental complexes **1a** and **2a** have been designed. The calculated results reveal that the different ancillary ligands in **1b-1d** and **2b-2d** stabilize the energy level of LUMOs more than that of HOMOs. Thus, the energy gap between HOMO and LUMO can be tuned. The lowest absorption bands for **1b-1d** (**2b-2d**) are blue-shifted compared with the parent complexes **1a** (**2a**). In addition, the calculated lowest energy emissions of **1b-1d** and **2b-2d** are at  $\sim 470$  nm with excellent blue light emitting properties. The higher quantum yield of **1a** compared with **2a** in the experiment was found to be closely related to smaller energy separation between the singlet  $S_1$  and the triplet  $T_3$  of the former. The smaller  $S_1-T_3$  energy difference for **1b**, **2b** and **2c** compared with that of **1a** and **2a** could blue shift the emission spectra and enhance the quantum efficiency. We suggest that a future experimental study on these high quantum yield complexes should be rewarding.

#### Acknowledgements

The authors thank the financial support from the National Natural Science Foundation of China (Grant no. 21273219, 21221061, 21203174), Natural Science Foundation of Jilin Province (20140101045JC).

## Notes and references

<sup>a</sup> College of Resource and Environmental Science, Jilin Agricultural University, Changchun, Jilin 130118, P. R. China.

<sup>b</sup> State Key Laboratory of Rare Earth Resource Utilization, Changchun Institute of Applied Chemistry, Chinese Academy of Sciences, Changchun 130022, P. R. China.

† Electronic Supplementary Information (ESI) available: Table S1: Main optimized geometry structural parameters of the complex **1a** in the ground at the DFT/PBE0, DFT/ B3LYP and DFT/ M062X level, respectively, together with the experimental values. Table S2: Calculated phosphorescent emission wavelength (nm)/energies (eV), of the complexes **1a** and **2a** in CH<sub>2</sub>Cl<sub>2</sub> media with the TDDFT method at the B3LYP, M062X and PBE0 level, respectively, together with the experimental values. Table S3: Calculated wavelength (nm), oscillator strength (*f*) and dominant orbital excitations of the lowest singlet and triplet absorptions for **2a-2d**. Table S4-S11: Molecular orbital composition (%) of **1a-1d** and **2a-2d** in the ground states. Table S12-S13: Optimized S<sub>0</sub> structures for the complexes **1a** and **2a**. See DOI: 10.1039/b000000x/

- 1 A. Tsuboyama, H. Iwawaki, M. Furugori, T. Mukaide, J. Kamatani, S. Igawa, T. Moriyama, S. Miura, T. Takiguchi, S. Okada, M. Hoshino and K. Ueno, *J. Am. Chem. Soc.*, 2003, **125**, 12971.
- 2 B. Du, C. Lin, Y. Chi, J. Y. Hung, M. W. Chung, T. Lin, G. H. Lee, K. T. Wong, P. T. Chou, W. Y. Hung and H. C. Chiu, *Inorg. Chem.*, 2010, **49**, 8713.
- 3 P. Vacca, M. Petrosino, A. Guerra, R. Chierchia, C. Minarini, D. Della Sala and A. Rubino, *J. Phys. Chem. C*, 2007, **111**, 17404.
- 4 Q. Zhao, M. Yu, L. Shi, S. Liu, C. Li, M. Shi, Z. Zhou, C. Huang and F. Li, *Organometallics*, 2010, **29**, 1085.
- 5 L. Xiong, Q. Zhao, H. Chen, Y. Wu, Z. Dong, Z. Zhou and F. Li, *Inorg. Chem.*, 2010, **49**, 6402.
- 6 C. Li, M. Yu, Y. Sun, Y. Wu, C. Huang and F. Li, *J. Am. Chem. Soc.*, 2011, **133**, 11231.
- 7 T. Yoshihara, Y. Yamaguchi, M. Hosaka, T. Takeuchi and S. Tobita, *Angew. Chem., Int. Ed.*, 2012, **51**, 4148.
- 8 (a) S. Zhang, M. Hosaka, T. Yoshihara, K. Negishi, Y. Iida, S. Tobita and T. Takeuchi, *Cancer Res.*, 2010, **70**, 4490; (b) R. D. Costa, E. Ortí, H. J. Bolink, F. Monti, G. Accorsi, and Ni. Armaroli, *Angew. Chem. Int. Ed.*, 2012, **51**, 8178; (c) F. Dumur, D. Bertin and D. Gimes, *Int. J. Nanotechnol.*, 2012, **9**, 377; (d) T. Hu, L. He, L. Duan and Y. Qiu, *J. Mater. Chem.*, 2012, **22**, 4206.
- 9 Y. Chi and P. T. Chou, *Chem. Soc. Rev.*, 2010, **39**, 638.
- 10 P. T. Chou and Y. Chi, *Chem. –Eur. J.*, 2007, **13**, 380.
- 11 Y. You, J. Seo, S. H. Kim, K. S. Kim, T. K. Ahn, D. Kim and S. Y. Park, *Inorg. Chem.*, 2008, **47**, 1476.
- 12 S. Tokito, T. Iijima, Y. Suzuri, H. Kita, T. Tsuzuki and F. Sato, *Appl. Phys. Lett.*, 2003, **83**, 569.
- 13 (a) W. Y. Wong and C. L. Ho, *Coord. Chem. Rev.*, 2009, **253**, 1709; (b) E. Holder, B. M. W. Langeveld and U. S. Schubert, *Adv. Mater.*, 2005, **17**, 1109.
- 14 C. Adachi, R. C. Kwong, P. Djurovich, V. Adamovich, M. A. Baldo, M. E. Thompson and S. R. Forrest, *Appl. Phys. Lett.*, 2001, **79**, 2082.
- 15 J. Li, P. I. Djurovich, B. D. Alleyne, M. Yousefuddin, N. N. Ho, J. C. Thomas, J. C. Peters, R. Bau and M. E. Thompson, *Inorg. Chem.*, 2005, **44**, 1713.
- 16 R. J. Holmes, B. W. D'Andrade, S. R. Forrest, X. Ren, J. Li and M. E. Thompson, *Appl. Phys. Lett.*, 2003, **83**, 3818.
- 17 M. Yeh, F. Wu, C. T. Chen, Y. H. Song, Y. Chi, M. H. Ho, S. F. Hsu and C. H. Chen, *Adv. Mater.*, 2005, **17**, 285.
- 18 S. Haneder, E. Da Como, J. Feldmann, J. M. Lupton, C. Lennartz, P. Erk, E. Fuchs, O. Molt, I. Münster, C. Schildknecht and G. Wagenblast, *Adv. Mater.*, 2008, **20**, 3325.
- 19 J. Y. Shen, C. Y. Lee, T. H. Huang, J. T. Lin, Y. T. Tao, C. H. Chien and C. J. Tsai, *J. Mater. Chem.*, 2005, **15**, 2455.
- 20 (a) S. O. Kim, K. H. Lee, G. Y. Kim, J. H. Seo, Y. K. Kim and S. S. Yoon, *Synth. Met.*, 2010, **160**, 1259; (b) C. H. Yang, M. Mauro, F. Polo, S. Watanabe, I. Muenster, R. Fröhlich, and L. D. Cola, *Chem. Mater.*, 2012, **24**, 3684; (c) F. Kessler, Y. Watanabe, H. Sasabe, H. Katagiri, Md. K. Nazeeruddin, M. Grätzel and J. Kido, *J. Mater. Chem. C*, 2013, **1**, 1070.
- 21 C. Fan, Y. H. Li, C. L. Yang, H. B. Wu, J. G. Qin, and Y. Cao, *Chem. Mater.*, 2012, **24**, 4581.
- 22 E. Runge and E. K. U. Gross, *Phys. Rev. Lett.*, 1984, **52**, 997.
- 23 (a) J. P. Perdew, K. Burke and M. Ernzerhof, *Phys. Rev. Lett.*, 1996, **77**, 3865; (b) J. P. Perdew, K. Burke and M. Ernzerhof, *Phys. Rev.*

- Lett.*, 1997, **78**, 1396; (c) C. Adamo and V. Barone, *J. Chem. Phys.*, 1999, **110**, 6158.
- 24 G. Zhou, C. L. Ho, W. Y. Wong, Q. Wang, D. Ma, L. Wang, Z. Lin, T. B. Marder and A. Beeby, *Adv. Funct. Mater.*, 2008, **18**, 499.
- 25 X. Li, Q. Zhang, Y. Tu, H. Ågren and H. Tian, *Phys. Chem. Chem. Phys.*, 2010, **12**, 13730.
- 26 C. L. Ho, Q. Wang, C. S. Lam, W. Y. Wong, D. Ma, L. Wang, Z. Q. Gao, C. H. Chen, K. W. Cheah and Z. Lin, *Chem. Asian J.*, 2009, **4**, 89.
- 27 (a) A. D. Becke, *J. Chem. Phys.*, 1993, **98**, 5648; (b) C. T. Lee, W. T. Yang and R. G. Parr, *Phys. Rev. B*, 1988, **37**, 785.
- 28 Y. Zhao and D. G. Truhlar, *Theor. Chem. Acc.*, 2008, **120**, 215.
- 29 (a) R. E. Stratmann, G. E. Scuseria and M. J. Frisch, *J. Chem. Phys.*, 1998, **109**, 8218; (b) N. N. Matsuzawa, A. Ishitani, D. A. Dixon and T. Uda, *J. Phys. Chem. A*, 2001, **105**, 4953.; (c) M. E. Casida, C. Jamorski, K. C. Casida and D. R. Salahub, *J. Chem. Phys.*, 1998, **108**, 4439.
- 30 (a) M. Cossi, G. Scalmani, N. Regar and V. Barone, *J. Chem. Phys.*, 2002, **117**, 43; (b) V. Barone, M. Cossi and J. Tomasi, *J. Chem. Phys.*, 1997, **107**, 3210.
- 31 (a) P. J. Hay and W. R. Wadt, *J. Chem. Phys.*, 1985, **82**, 270; (b) W. R. Wadt and P. J. Hay, *J. Chem. Phys.*, 1985, **82**, 284; (c) P. J. Hay and W. R. Wadt, *J. Chem. Phys.*, 1985, **82**, 299.
- 32 P. C. Hariharan and J. A. Pople, *Mol. Phys.*, 1974, **27**, 209.
- 33 M. J. Frisch, G. W. Trucks, H. B. Schlegel, G. E. Scuseria, M. A. Robb, J. R. Cheeseman, G. Scalmani, V. Barone, B. Mennucci, G. A. Petersson, H. Nakatsuji, M. Caricato, X. Li, H. P. Hratchian, A. F. Izmaylov, J. Bloino, G. Zheng, J. L. Sonnenberg, M. Hada, M. Ehara, K. Toyota, R. Fukuda, J. Hasegawa, M. Ishida, T. Nakajima, Y. Honda, O. Kitao, H. Nakai, T. Vreven, J. A. Montgomery, Jr, J. E. Peralta, F. Ogliaro, M. Bearpark, J. J. Heyd, E. Brothers, K. N. Kudin, V. N. Staroverov, T. Keith, R. Kobayashi, J. Normand, K. Raghavachari, A. Rendell, J. C. Burant, S. S. Iyengar, J. Tomasi, M. Cossi, N. Rega, J. M. Millam, M. Klene, J. E. Knox, J. B. Cross, V. Bakken, C. Adamo, J. Jaramillo, R. Gomperts, R. E. Stratmann, O. Yazyev, A. J. Austin, R. Cammi, C. Pomelli, J. W. Ochterski, R. L. Martin, K. Morokuma, V. G. Zakrzewski, G. A. Voth, P. Salvador, J. Dannenberg, S. Dapprich, A. D. Daniels, O. Farkas, J. B. Foresman, J. V. Ortiz, J. Cioslowski and D. J. Fox, Gaussian **09**, Revision B.01, Gaussian, Inc., Wallingford, CT, 2010
- 34 N. M. O'Boyle, A. L. Tenderholt and K. M. Langner, *J. Comput. Chem.*, 2008, **29**, 839.
- 35 U. Varetto, MOLEKEL Version, Swiss National Supercomputing Centre, Lugano Switzerland.
- 36 (a) A. Dreuw and M. Head-Gordon, *Chem. Rev.*, 2005, **105**, 4009; (b) M. K. Nazeeruddin, F. D. Angelis, S. Fantacci, A. Selloni, G. Viscardi, P. Liska, S. Ito, B. Takeru and M. Gratzel, *J. Am. Chem. Soc.*, 2005, **127**, 16835; (c) D. Jacquemin, E. A. Perpète, G. E. Scuseria, I. Cifini and C. Adamo, *J. Chem. Theory. Comput.*, 2008, **4**, 123; (d) Q. Cao, J. Wang, Z. S. Tian, Z. F. Xie and F. Q. Bai, *J. Comput. Chem.*, 2012, **33**, 1038; (e) Y. L. Si, Y. Q. Liu, X. C. Qu, Y. Wang and Z. J. Wu, *Dalton Trans.*, 2013, **42**, 14149.
- 37 (a) X. Li, Q. Zhang, Y. Q. Tu, H. Ågren and H. Tian, *Phys. Chem. Chem. Phys.*, 2010, **12**, 13730; b) L. L. Shi, J. J. Su and Z. J. Wu, *Inorg. Chem.*, 2011, **50**, 5477.
- 38 J. D. Chai and M. Head-Gordon, *Phys. Chem. Chem. Phys.*, 2008, **10**, 6615.
- 39 (a) S. Sprouse, K. A. King, P. J. Spellane and R. J. Watts, *J. Am. Chem. Soc.*, 1984, **106**, 6647; (b) M. G. Colombo, T. C. Brunold, T. Riedener, H. U. Güdel, M. Förtsch and H. B. Bürgi, *Inorg. Chem.*, 1994, **33**, 545.
- 40 (a) P. Jeffrey Hay, *J. Phys. Chem. A*, 2002, **106**, 1634; (b) A. R. G. Smith, M. J. Riley, S. C. Lo, P. L. Burn, I. R. Gentle and B. J. Powell, *Phys. Rev. B*, 2011, **83**, 041105.
- 41 I. Avilov, P. Minoofar, J. Cornil and L. De Cola, *J. Am. Chem. Soc.*, 2007, **129**, 8247.
- 42 D. N. Kozhevnikov, V. N. Kozhevnikov, M. Z. Shafikov, A. M. Prokhorov, D. W. Bruce and J. A. Gareth Williams, *Inorg. Chem.*, 2011, **50**, 3804.
- 43 C. H. Yang, Y. M. Cheng, Y. Chi, C. J. Hsu, F. C. Fang, K. T. Wong, P. T. Chou, C. H. Chang, M. H. Tsai and C. C. Wu, *Angew. Chem., Int. Ed.*, 2007, **46**, 2418.
- 44 (a) G. Gigli, F. Della Sala, M. Lomascolo, M. Anni, G. Barbarella, A. Di Carlo, P. Lugli and R. Cingolani, *Phys. Rev. Lett.*, 2001, **86**, 167;

(b) D. Beljonne, J. Cornil, R. H. Friend, R. A. J. Janssen and J. L. Brédas, *J. Am. Chem. Soc.*, 1996, **118**, 6453; (c) A. L. Burin and M. A. Ratner, *J. Chem. Phys.*, 1998, **109**, 6092.